 DOI: 10.19601/j.cnki.issn1943 - 9903.2024.05.004

Feasibility Evaluation of Using Biochar-based Permeable Reactive Barrier for the Remediation of Mercury and Arsenic Composite Polluted Water Bodies

Dilixiati · Abulizi *

Urumqi Vocational University, Urumqi 830001, China

Abstract This study employed a modified biochar material to construct a permeable reactive barrier (PRB) for the treatment of water bodies polluted with mercury and arsenic. The experimental results demonstrated that the addition of goethite-modified biochar significantly enhanced the remediation efficiency of As (III), achieving a maximum removal rate of 100%. Conversely, pure biochar exhibited high efficiency in the removal of Hg (II), with a maximum removal rate approaching 100%. Furthermore, the pH level of the water significantly influenced the adsorption efficiency of heavy metal ions, with the optimal removal performance observed at a pH of 6.0. The PRB system demonstrated excellent removal rates under low concentrations of heavy metals. However, as the concentration increased, the remediation efficiency exhibited a slight decrease. In summary, the findings of this study provide compelling evidence for the use of modified biochar in the construction of PRBs for the remediation of mercury and arsenic-polluted water bodies. Furthermore, the study reveals the mechanism by which pH and heavy metal concentration influence remediation efficiency.

Key words Biochar, Goethite-modified biochar, Permeable reactive barrier (PRB), Mercury and arsenic pollution, Remediation efficiency

1 Introduction

Heavy metal ions are highly toxic, accumulate in large quantities, and are extremely harmful to humans and the environment[1]. They are non-biodegradable, stable, and persistent, and have diverse forms, with a variety of ions often coexisting, making their removal difficult. A variety of technologies have been employed to treat heavy metal ions in wastewater[1-2], including adsorption[3-6], chemical precipitation[7-8], ion exchange[9-10], and membrane treatment[11-13]. These methods have both advantages and disadvantages in the treatment of heavy metal wastewater. However, they are not effective in the treatment of coexisting heavy metal ions, particularly when anions and cations coexist[14]. Therefore, it is of great importance to identify efficient and economical methods for the removal of heavy metal ions.

The removal of heavy metal ions has emerged as a significant area of research interest. The permeable reactive barrier (PRB) technology has emerged as a promising approach for the remediation of heavy metal-polluted water, due to its cost-effectiveness, high efficiency, and environmental compatibility[15-16]. This technology employs an in situ permeable reaction medium to treat polluted groundwater. This approach allows for the removal of contaminants in situ, thereby reducing costs. PRB technology is particularly advantageous for groundwater contamination remediation, as it minimizes operation and maintenance costs compared to surface treatment of large quantities of low concentration water[17-18].

The reaction medium plays a pivotal role in determining the efficacy and longevity of PRB systems. The selection of an optimal reaction medium should be guided by considerations such as activity, permeability or hydraulic conductivity, environmental compatibility, availability, cost, and long-term stability[19].

This study investigated the performance of goethite biochar mixtures in PRB columns for the remediation of mercury and arsenic polluted water bodies. The specific aims were to examine the removal effects of the mixtures on mercury and arsenic, analyze the effects of pH and initial concentration on the removal effect, and reveal the removal mechanism of mercury and arsenic by the mixture.

2 Materials and methods

2.1 Materials The cotton straw biochar was obtained from the Xinjiang Academy of Agricultural Sciences. The pretreatment process involved soaking the material in 5% hydrochloric acid for 24 h, washing it with deionized water to achieve a pH of 7.0, drying it at 60 ℃ for 24 h, and storing it in a desiccator for future use.

Regarding the synthesis of goethite biochar composite, the following adjustments were made: the ratio of the raw materials was altered to 1∶1, with the mass ratio of $Fe(NO_3)_3 \cdot 9H_2O$ to biochar adjusted to 1∶1. Other synthesis conditions were maintained throughout the experiment, with the pH of the mixture adjusted to approximately 12 using a 5M KOH solution, followed by aging at a temperature of 60 ℃ for 60 h. Following the completion of the synthesis, the goethite biochar composites were rinsed with deionized water until the pH of the supernatant was nearly neutral (approximately 7.0).

Received: January 15, 2024 Accepted: April 10, 2024

* Corresponding author. Dilixiati · Abulizi, PhD., associate professor, research fields: bioremediation of environmental pollution.

2.2 PRB column test A plexiglass column was utilized to construct a simulated PRB system under laboratory conditions (Fig. 1). The PRB reaction column was designed from plexiglass with a length of 20 cm and an internal diameter of 4.4 cm. The specific design parameters are shown in Fig. 1.

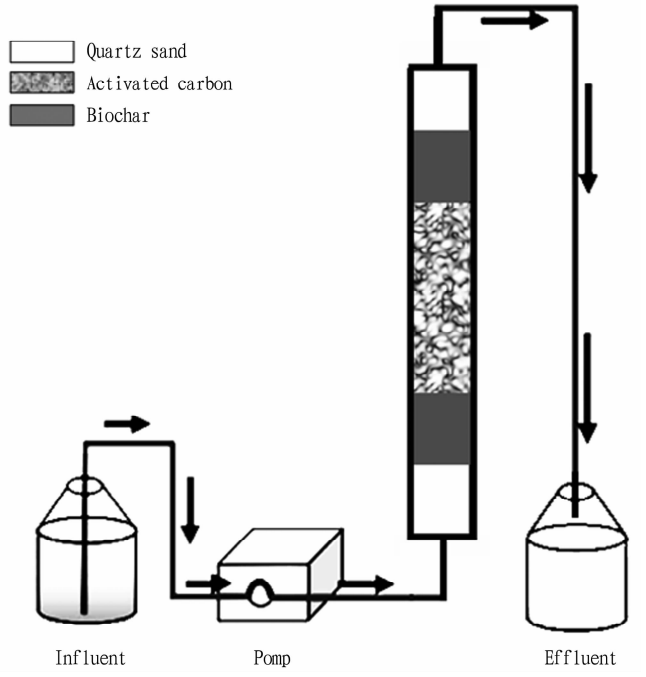

Fig. 1 Schematic diagram of experimental setup

The first step involved the filling of the column with 50 g of goethite biochar composite. This composite was screened through a 60-mesh sieve with a particle size of approximately 0.250 mm and a length of 4.0 cm after filling. Subsequently, 20 g of activated carbon was introduced above and below the goethite biochar composite. The activated carbons had a particle size of approximately 0.3 – 0.5 mm and a total length of 3.0 cm after filling.

Finally, to complete the entire system, it is necessary to fill the upper and lower portions of the column with 60 g of quartz sand (particle size 2 – 5 mm, height 3.5 cm). This serves as a filtration, buffer, and protection medium. As outlined in the literature[20-22], the incorporation of activated carbon between the media of the PRB system serves to enhance the pollutant removal effect. The judicious selection of media components enables the construction of an efficient and stable PRB system, capable of meeting the diverse demands of treatment.

A simulated wastewater with a composite pollution of Hg (II) and As (III) was employed as the flow environment, wherein the concentration of both Hg (II) and As (III) was 10 mg/L. The core medium, comprising goethite biochar composite, was fully mixed with activated carbon and quartz sand in a fixed ratio and then filled into the reactor. The test was conducted in two stages: the first stage involved the simulation of the treatment of arsenic-containing wastewater, while the second stage simulated the treatment of mercury-containing wastewater. In each stage, water samples were filled into Mariotte bottles and passed through the reactor at a flow rate of 1 mL/min.

Following the stabilization of the effluent, water samples were collected and filtered through a 0.22 μm membrane. The mercury and arsenic contents were then determined by an AFS-810 atomic fluorescence photometer (AFS-810, Jitian, Beijing, China). The removal rate was calculated based on the concentration difference between the influent and effluent to evaluate the treatment effect of the reactor.

3 Results and analysis

3.1 Remediation performance of biochar PRB on mercury and arsenic composite polluted water bodies

3.1.1 Remediation of mercury and arsenic composite pollution by biochar PRB using different reactive materials. Three PRB columns were constructed with biochar (50 g), a biochar and goethite modified biochar mixture (25 g each), and goethite modified biochar (50 g), which were labeled BC, BC + GBC, and GBC, respectively. In order to simulate the actual multi-component pollution, a simulated water body containing As (III) and Hg (II), both at a concentration of 10 mg/L, was configured. The simulated sewage was treated at pH 6.0, a flow rate of 1.0 mL/min, and 25 ℃, and the removal results are shown in Fig. 2. It is evident that there are differences in the removal capacity of PRB systems constructed with different reactive materials. These results can provide a reference for optimizing system design and operation.

The removal efficiency of As (III) and Hg (II) by the three PRB systems was satisfactory. At 120 h, the removal rates of As (III) by BC (Fig. 2a), BC + GBC (Fig. 2b), and GBC (Fig. 2c) were 85.7%, 93.8%, and 100%, respectively. Similarly, the removal rate of Hg (II) was close to 100% in all cases. The removal rate of As (III) by pure biochar was low, but the removal rate was increased by the mixing of goethite-modified biochar. The PRB constructed with pure goethite-modified biochar demonstrated 100% removal rate of As (III). The three PRBs demonstrated high Hg (II) removal rate, with the highest observed in the pure biochar sample. The final Hg (II) concentration in the effluent after 120 h was below the limit of detection, at 0 mg/L.

In this study, the goethite-modified biochar, prepared to optimal specifications, was utilized to construct the PRB, which was then employed to treat simulated arsenic polluted water bodies. The results demonstrated a maximum removal rate of 100%, which is an ideal medium for As adsorption.

3.1.2 Remediation of composite mercury and arsenic pollution by biochar PRB at different pH. In the multicomponent system, the simulated polluted water contained 10 mg/L As (III) and Hg (II). The results of As (III) and Hg (II) removal by the PRB system constructed with goethite-modified biochar at a flow rate of 1.0 mL/min and a temperature of 25 ℃ with an initial pH of 3.0, 6.0, and 9.0 are shown in Fig. 3.

The pH significantly influenced the removal efficiency of metals in the PRB. The residual concentrations of As (III) were 0.30, 0.00 and 0.80 mg/L, while those of Hg (II) were 0.13, 0.002 and 0.29 mg/L, respectively, after 120 h of treatment at pH 3.0, 6.0 and 9.0, respectively. The optimal performance for the

removal of As (III) and Hg (II) was observed in the PRB constructed with goethite-modified biochar at a pH of 6.0. Observation of Fig. 3d revealed that the pH of the effluent from the PRB treatment process exhibited temporal fluctuations when the initial pH of the water body was 3.0. The change in pH is intimately associated with the extent of adsorption of heavy metal ions by the PRB media.

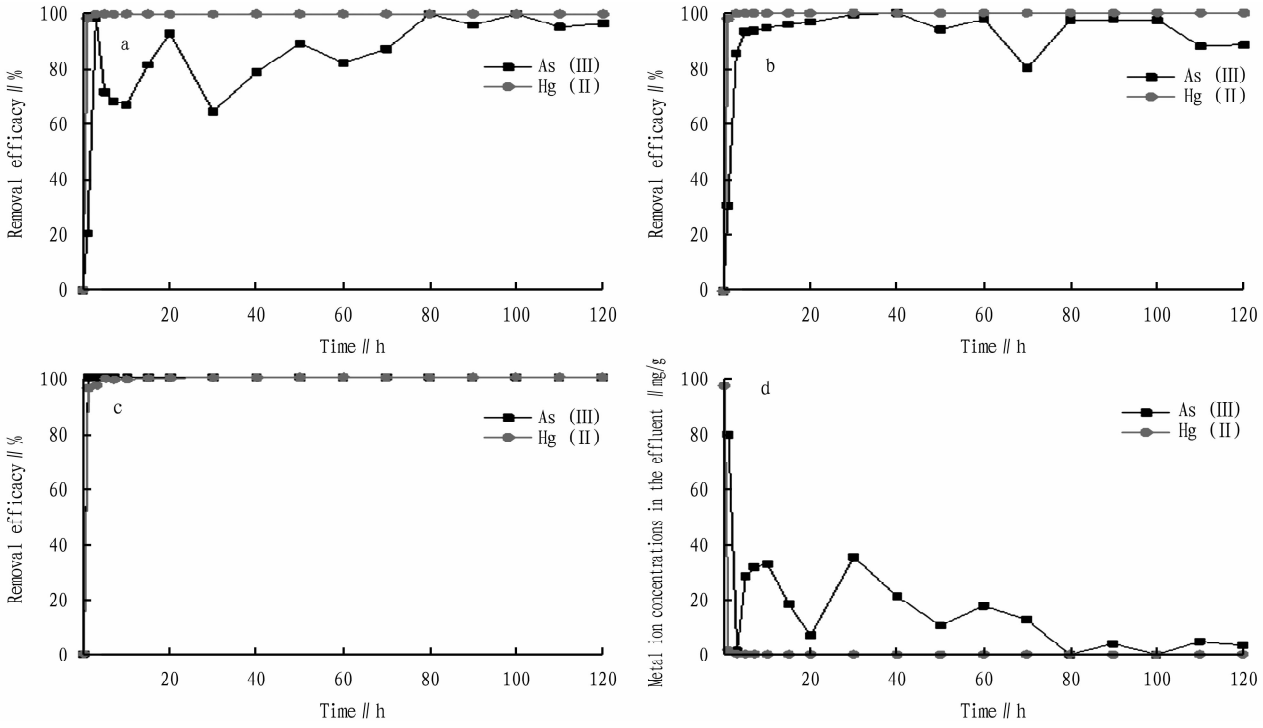

NOTE a. 50 g BC; b. 25 g BC + 25 g GBC; c. 50 g GBC; d. Metal ion concentrations in the effluent for 50 g BC used as PRB medium. Heavy metal initial concentration, 10.0 mg/L; flow rate, 1.0 mL/min; initial pH, 6.0.

Fig. 2 Effect of different reactive materials used in PRBs on the removal of heavy metal ions

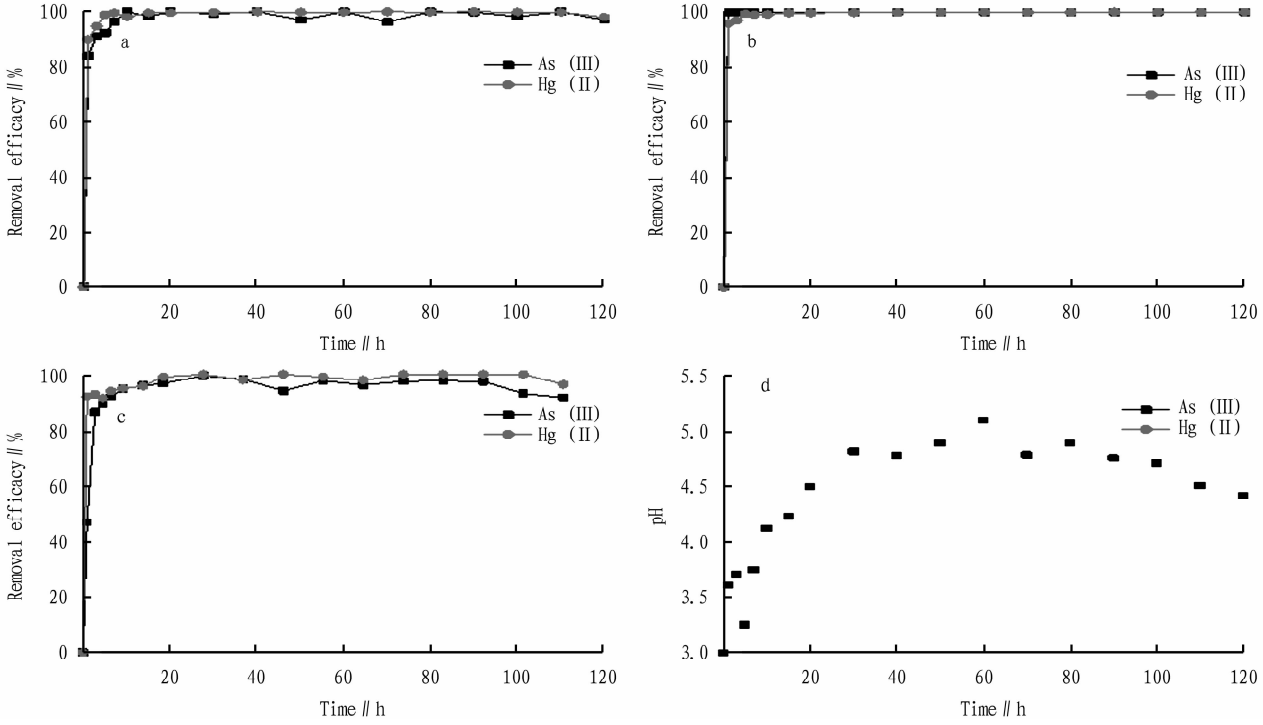

NOTE a. pH = 3.0; b. pH = 6.0; c. pH = 9.0; d. pH changes in the effluents at initial pH of 3.0. Heavy metal initial concentration, 10.0 mg/L; flow rate, 1.0 mL/min; PRB medium, GBC 50 g.

Fig. 3 Effect of pH on the removal of heavy metal ions

3.2 Remediation performance of biochar PRB for mercury/arsenic polluted water bodies in a single component system

3.2.1 Remediation of arsenic polluted water body by biochar PRB at different initial arsenic concentrations. In the single component system, different concentrations of simulated polluted water bodies were configured. The concentrations of As (III) or Hg (II) were set at 5.0, 10.0 and 20.0 mg/L, respectively. In the experimental phase, the water flow rate was maintained at 1.0 mL/min, the temperature at 25 ℃, and the initial pH of the effluents was set at 6.0. The results of the treatment are presented in Figs.4-5, respectively.

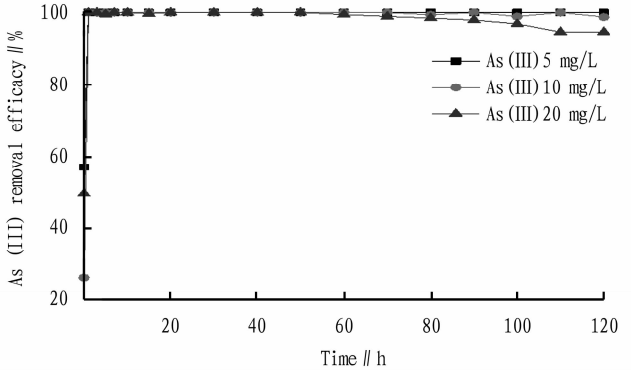

Fig.4 Removal efficiency of biochar PRB under different initial As (III) concentrations

Fig.4 illustrates that the PRB system exhibited an over 99% removal rate and high efficiency when the initial concentrations of As (III) were 5.0 and 10.0 mg/L. Upon increasing the concentration to 20 mg/L, the removal rate exhibited a slight decline to 98.83%. However, this value remained close to 100%, indicating that the PRB system retained its efficient removal capability for high As (III) concentrations. Following 120 h of treatment, the remaining concentration of As (III) in the PRB column was observed. Nearly complete removal of As (III) was observed at initial concentrations of 5.0 and 10.0 mg/L, with concentrations of 0 and 0.12 mg/L, respectively. 1.06 mg/L remained at an initial concentration of 20.0 mg/L, but the removal rate was still high.

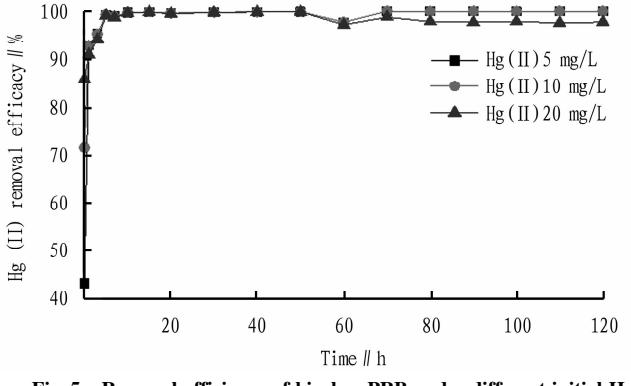

Fig.5 Removal efficiency of biochar PRB under different initial Hg (II) concentrations

3.2.2 Remediation of arsenic polluted water body by biochar PRB at different initial mercury concentrations. Fig.5 illustrates that at initial concentrations of 5.0 and 10.0 mg/L, the removal rate of Hg (II) by the PRB system was over 98.9%, which was highly efficient and stable. At the initial concentration of 20.0 mg/L, the removal rate exhibited a slight decrease to 97.98%, yet the treatment capacity remained robust. After 120 h of treatment, the remaining concentration of Hg (II) in the PRB column was observed. At the initial concentration of 5.0 mg/L, 0.001 mg/L remained; at 10.0 mg/L, 0.003 mg/L remained, representing a near complete removal. At 20.0 mg/L, 0.454 mg/L remained, yet the removal rate remained considerable. The PRB system, comprising goethite-modified biochar, demonstrated efficacy at varying Hg (II) concentrations, thus offering an efficacious approach for the remediation of Hg (II)-laden wastewater.

4 Conclusions

This study employed a modified biochar to construct PRBs for the purpose of treating water body contaminated with mercury and arsenic. The experimental results are as follows.

(i) An increase in the proportion of goethite-modified biochar resulted in enhanced As (III) remediation, with a maximum removal rate of 100%. Furthermore, the higher the pure biochar content, the greater the Hg (II) removal rate, reaching a maximum of 99.99%.

(ii) The pH exhibited a pronounced influence on the heavy metal adsorption efficiency, with the optimal removal performance observed at pH 6.0.

(iii) At initial concentrations of 5.0 and 10.0 mg/L, the removal rate was over 99%. When the concentration was increased to 20.0 mg/L, the removal rate decreased slightly, but remained efficient. This indicates that the PRB system can effectively treat mercury and arsenic pollution despite the decrease in remediation efficiency at high concentrations.

References

[1] BERMUDEZ GA, JASAN R, PLÁ R, *et al.* Heavy metal and trace element concentrations in wheat grains: Assessment of potential non-carcinogenic health hazard through their consumption[J]. Journal of Hazardous Materials, 2011(193): 264-271.

[2] FU FL, WANG Q. Removal of heavy metal ions from wastewaters: A review[J]. Environmental Management, 2011(92): 407-418.

[3] HUA M, ZHANG SJ, PAN BC, *et al.* Heavy metal removal from water/wastewater by nanosized metal oxides: A review[J]. Journal of Hazardous Materials, 2012(211-212): 317-331.

[4] YANG GX, JIANG H. Amino modification of biochar for enhanced adsorption of copper ions from synthetic wastewater[J]. Water Research, 2014(48): 396-405.

[5] REPO E, WARCHOŁ JK, BHATNAGAR A, *et al.* Aminopolycarboxylic acid functionalized adsorbents for heavy metals removal from water[J]. Water Research, 2013(47): 4812-4832.

[6] AHMAD M, RAJAPAKSHA AU, LIM JE, *et al.* Biochar as a sorbent for

contaminant management in soil and water: A review[J]. Chemosphere, 2014(99): 19 – 33.
[7] MEUNIER N, DROGUI P, MONTANÉ C, *et al.* Comparison between electrocoagulation and chemical precipitation for metals removal from acidic soil leachate[J]. Journal of Hazardous Materials, 2006(137): 581 – 590.
[8] MATLOCK MM, HOWERTON BS, ATWOOD DA. Chemical precipitation of heavy metals from acid mine drainage[J]. Water Research, 2002(36): 4757 – 4764.
[9] RUDNICKI P, HUBICKI Z, KOŁODYNSKA D. Evaluation of heavy metal ions removal from acidic waste water streams[J]. Chemical Engineering Journal, 2014(252): 362 – 373.
[10] AZARUDEEN RS, SUBHA R, JEYAKUMAR D, *et al.* Batch separation studies for the removal of heavy metal ions using a chelating terpolymer: synthesis, characterization and isotherm models[J]. Separation and Purification Technology, 2013(116): 366 – 377.
[11] GAO J, SUN SP, ZHU WP, *et al.* Chelating polymer modified P84 nanofiltration (NF) hollow fiber membranes for high efficient heavy metal removal[J]. Water Research, 2014(63): 252 – 261.
[12] ALGARRA M, VáZQUEZ MI, ALONSO B, *et al.* Characterization of an engineered cellulose based membrane by thiol dendrimer for heavy metals removal[J]. Chemical Engineering Journal, 2014(253): 472 – 477.
[13] QIU YR, MAO LJ. Removal of heavy metal ions from aqueous solution by ultra filtration assisted with copolymer of maleic acid and acrylic acid [J]. Desalination, 2013(329): 78 – 85.
[14] HA WJ, FU FL, CHENG ZH, *et al.* Studies on the optimum conditions using acid-washed zero-valent iron/aluminum mixtures in permeable reactive barriers for the removal of different heavy metal ions from wastewater[J]. Journal of Hazardous Materials, 2016(302): 437 – 446.
[15] WOINARSKI AZ, STEVENS GW, SNAPE I. A natural zeolite permeable reactive barrier to treat heavy-metal contaminated waters in Antarctica: kinetic and fixed-bed studies, Process Safety and Environmental Protection, 2006(84): 109 – 116.
[16] DONG J, ZHAO YS, ZHANG WH, *et al.* Laboratory study on sequenced permeable reactive barrier remediation for landfill leachate-contaminated groundwater [J]. Journal of Hazardous Materials, 2009(161): 224 – 230.
[17] HAN YS, GALLEGOS TJ, DEMOND AH, *et al.* FeS-coated sand for removal of arsenic (III) under anaerobic conditions in permeable reactive barriers[J]. Water Research, 2011(45): 593 – 604.
[18] HENDERSON AD, DEMOND AH. Permeability of iron sulfide (FeS)-based materials for groundwater remediation[J]. Water Research, 2013(47): 1267 – 1276.
[19] DILIXIATI. Effect of preparation conditions of goethite biochar composite on mercury and arsenic adsorption properties[J]. Chemical Reagents, 2021, 43(5): 590 – 597. (In Chinese).
[20] NEUMANN A, KAEGI R, VOEGELIN A, *et al.* Arsenic removal with composite iron matrix filters in Bangladesh: A field and laboratory study [J]. Environmental Science & Technology, 2013(47): 4544 – 4554.
[21] YANG J, GUO Y, XU D, *et al.* A controllable Fe0-C permeable reactive barrier for 1,4-dichlorobenzene dechlorination[J]. Chemical Engineering Journal, 2012(203): 166 – 173.
[22] ZHOU D, LI Y, ZHANG Y, *et al.* Column test-based optimization of the permeable reactive barrier(PRB) technique for remediating groundwater contaminated by landfill leachates[J]. Journal of Contaminant Hydrology, 2014(168): 1 – 16.

(From page 14)

mal utilization of resources and the balanced advancement of the north and south sections in their current state.

References

[1] LIU JC. Optimization of mining program in over-anticline area of Antaibao Open-pit Coal Mine[J]. Opencast Mining Technology, 2023, 38(3): 92 – 96. (in Chinese).
[2] HUANG KJ, LI JG, FU HL, *et al.* optimization of mining procedure under the condition of limited land use in Baiyinhua No.3 mine[J]. China Coal Industry, 2020(S1): 38 – 39. (in Chinese).
[3] LIU C, BAI RC, LIU GW, *et al.* Optimization of mining sequence based on coordination mining technology between two adjacent open pits[J]. Journal of Chongqing University, 2016, 39(4): 103 – 111. (in Chinese).
[4] FENG ZL. Mining sequence optimization in Biesikuduke open-pit coal mine[J]. Opencast Mining Technology, 2019, 34(3): 58 – 61. (in Chinese).
[5] ZHAO HZ, LI ZW, SUN JD, *et al.* Optimization of mining sequence in the fault-subsiding area of Heidaigou open-pit mine[J]. Journal of Mining Science and Technology, 2020, 5(2): 187 – 193. (in Chinese).
[6] BAI RC, LIU YX, LIU GW, *et al.* Optimization of open-pit mining process based on improved AHP comprehensive evaluation method[J]. Journal of Liaoning Technical University (Natural Science), 2018, 37(3): 462 – 468. (in Chinese).
[7] ZHAO HZ, ZHENG QF, ZHAO BS. Research on the coordination mining patterns of open-pit mine group[J]. Opencast Mining Technology, 2017, 32(9): 1 – 5. (in Chinese).
[8] LIU JY, SHI J, LIU ZH, *et al.* Study on coordinated mining schemes of Huolinhe South and North Open-pit Mine[J]. Opencast Mining Technology, 2023, 38(3): 58 – 61. (in Chinese).
[9] LIU JY, SHI J, LIU ZH, *et al.* Optimization of mining technology and equipment layout in Huolinhe North Open-pit Mine[J]. Opencast Mining Technology, 2023, 38(1): 72 – 75, 78. (in Chinese).
[10] GUO HJ, LI M, CHENG G, *et al.* Study on control mining scheme for east slope of north area in Huolinhe South Open-pit Coal Mine[J]. Opencast Mining Technology, 2023, 38(4): 74 – 77. (in Chinese).